Appendix

A1: Fractal dimensions

Table A1. Fractal dimensions were calculated from the local fractal dimension *vs*. frequency plot using the box-counting method through the FE-SEM images.

Concentration	Fractal Dimension
1 wt.% (24 h)	1.83 1.94 1.98
1 wt.% (48 h)	1.84 1.96
2 wt.% (48 h)	1.79 1.93 1.98
4 wt.% (48 h)	1.60 1.83 1.90 1.96

A2: Tensile measurements

Stress-strain plots of pure NaCMC, un-irradiated (0 kGy) and irradiated WS_2 at 10 kGy and 35 kGy. The ultimate tensile stress (MPa), elongation (%), and modulus (MPa) of pure NaCMC films are 3.59 MPa, 206 5, and 0.508 MPa, respectively.

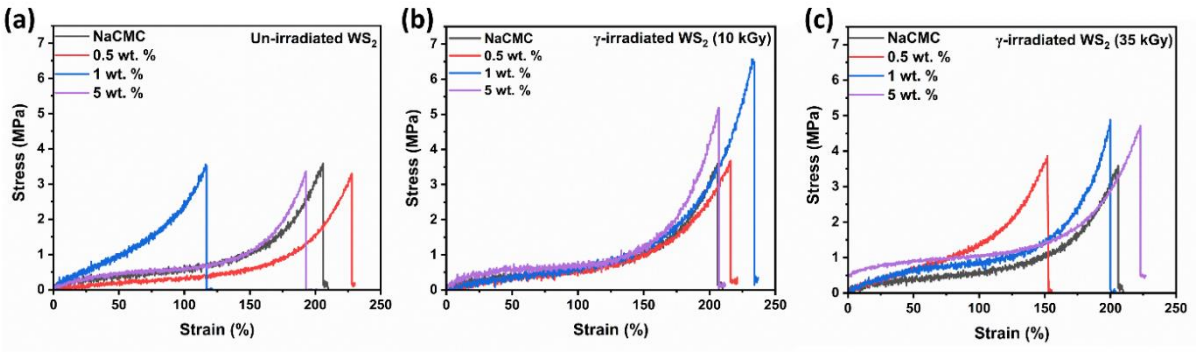

Figure A1: Stress *vs*. strain plot at a strain rate of 5 mm/min of WS_2/NaCMC nanocomposite films are plotted for (a) un-irradiated WS_2, and γ-irradiated WS_2 at (b) 10 kGy, (c) 35 kGy for pure NaCMC and different concentrations of WS_2/NaCMC nanocomposite films at 5 wt.%, 1 wt.% and 5 wt.%.

A3: β-decay mechanism

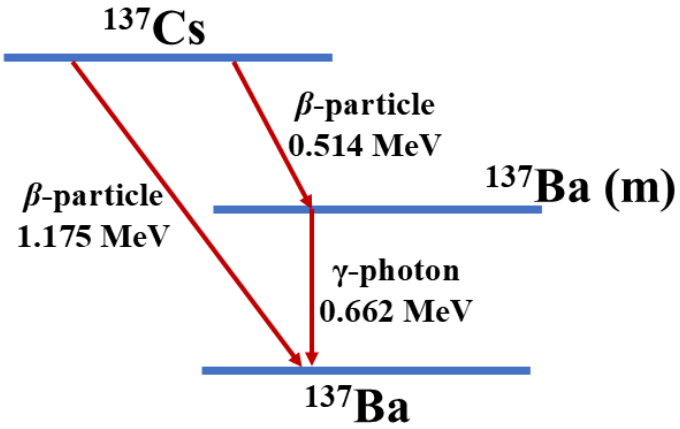

Figure A2: Decay scheme of β-source (Cesium-137).

A4: Raman spectra of β-irradiated WS_2 system

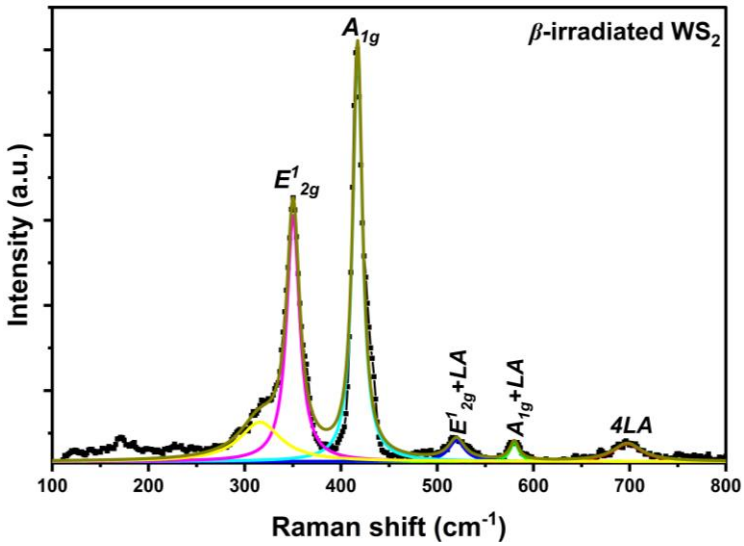

Figure A3: Deconvoluted Raman spectra of β-irradiated WS_2 system fitted with a Lorentzian function.

A5: Pore size distribution analysis using BJH model

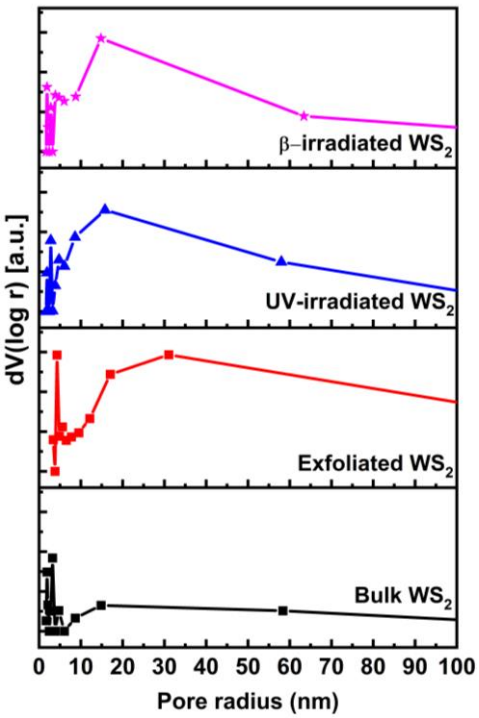

Figure A4: Pore size distributions of bulk WS_2, exfoliated WS_2, UV- and β-irradiated WS_2.

A6: Schematic representation of 15 keV He^{2+} irradiated WS_2 system at normal and oblique angle incidence

Schematic diagram of normal (vertical) incidences making an angle of 0° onto the sample surface and oblique angle incidences, that was placed on a 35° slanting stand, creating a 55° angle between the incoming beam and the sample surface as shown in the scheme below.

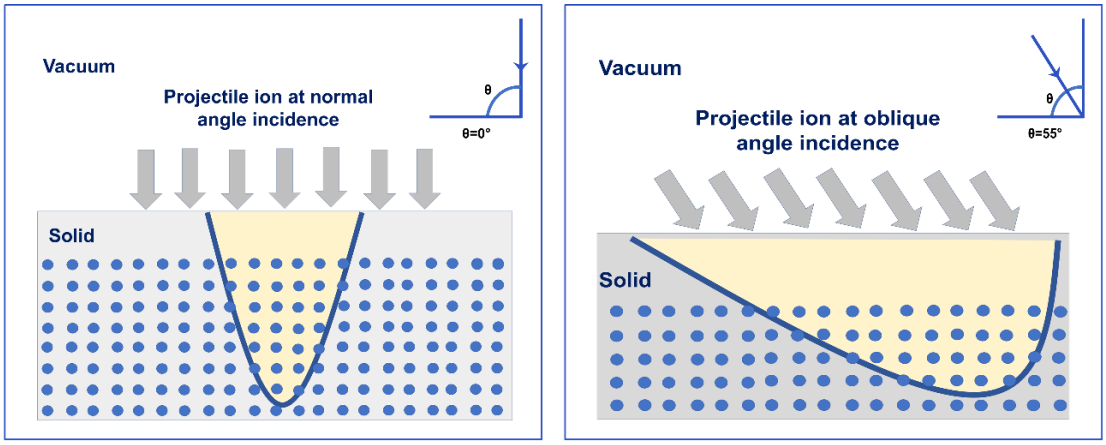

Figure A5: The schematic representation of normal (0°) and oblique angle incidence (55°) of projectile ions.

A7: AFM details

The surface topography of the films was exploited by an atomic force microscope (AFM, NTEGRA Prima®, ND-MDT Technology). The scanning was done in a semi-contact mode with a Si tip of dia. 10 nm and with 2.5×2.5 μm^2 scan area.

A8: SRIM/TRIM calculation details

The effects of collision cascades caused by ion irradiation were studied using TRIM calculations, which trace the trajectory of each recoil atom until its energy falls below the displacement threshold of the target atoms. In a WS_2 target, an energetic incident ion generates a primary knock-on atom (PKA), which then initiates a cascade of atomic displacements. This process results in the creation of vacancies and interstitial atoms. For 15 keV He^{2+} and 15 keV C^{2+} ions, calculations were carried out considering ~99,999 atoms and a depth window of ~5000 Å to predict the projectile ion range, ion concentration and distribution profile, straggling effect and damage events, etc. TRIM simulations were carried out for U^{28+} ions in a WS_2 target, considering full damage cascades involving ~5,000 atoms. The simulation utilized a plot window of ~40 µm and a cell width of 4000 Å.

Here, WS_2 is the target matter whose density, considered for TRIM calculations, is 7.83 g/cm^3, and the displacement energy of W and S in WS_2 is ~25 eV. In the WS_2 system, tungsten (W) constitutes 33.3% of the atomic composition and 74.1% of the mass, while sulfur (S) makes up 66.6% of the atomic composition and 25.8% of the mass. Throughout the calculation, the stoichiometric ratio of W to S in WS_2 was maintained at 1:2.

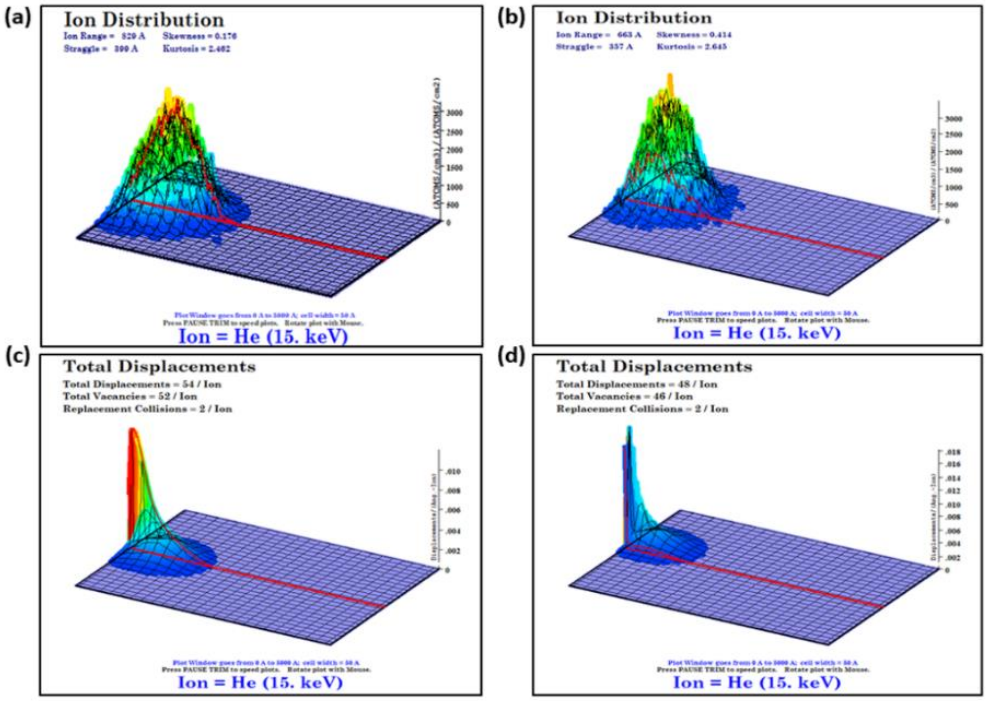

Figure A6: SRIM/TRIM simulations of 15 keV He ions in WS_2, (a,b) Ion distribution profile, (c,d) total displacements/vacancies created with plot windows of depth 0 Å to 5000 Å (towards right) for 0° and 55º incident angle, respectively. The red and cyan colour in the figure represent the moving atoms, while the stopping atoms are denoted by green and blue. Note that the plot window is considered up to a depth of 5000 Å, as the incident ions penetrate from the left onto a target.

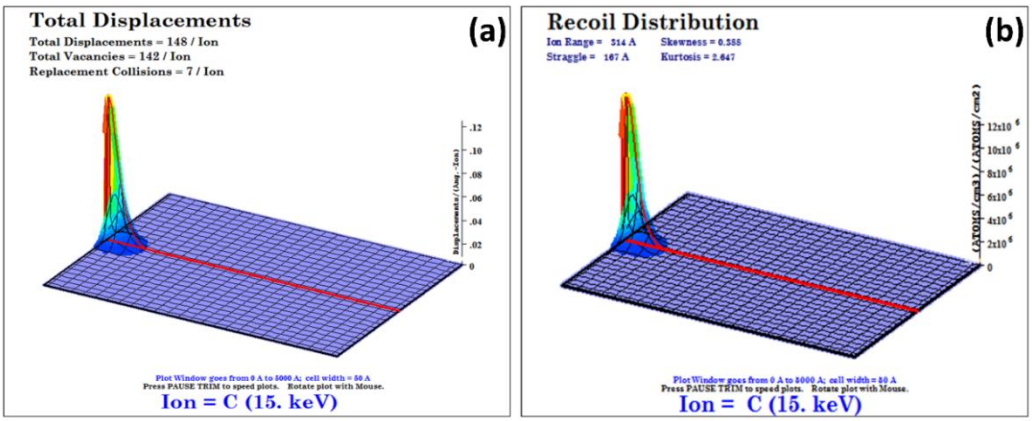

Figure A7: SRIM/TRIM calculation with 15 keV C^{2+} ion irradiation, 3D plots of (a) target displacements and (b) recoil distribution *vs.* target depth. Note that the plot window is considered up to a depth of 5000 Å, as the incident ions penetrate from the left onto a target.

A9: Migration barrier calculations

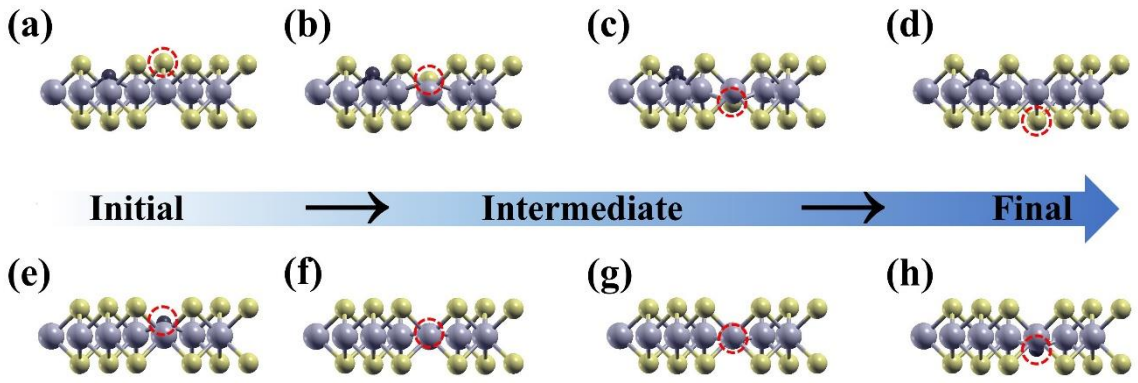

Figure A8: Migration of S (a-d) and C (e-h) atoms in the WS_2 system. Panels (a–d) and (e–h) illustrate the initial, intermediate (4^{th} and 7^{th} out of 10 total images), and final stages of the migration process for sulfur and carbon atoms, respectively.

A10: XPS survey scans of bulk and exfoliated WS_2 before and after irradiation with 0.85 GeV U^{28+} ions

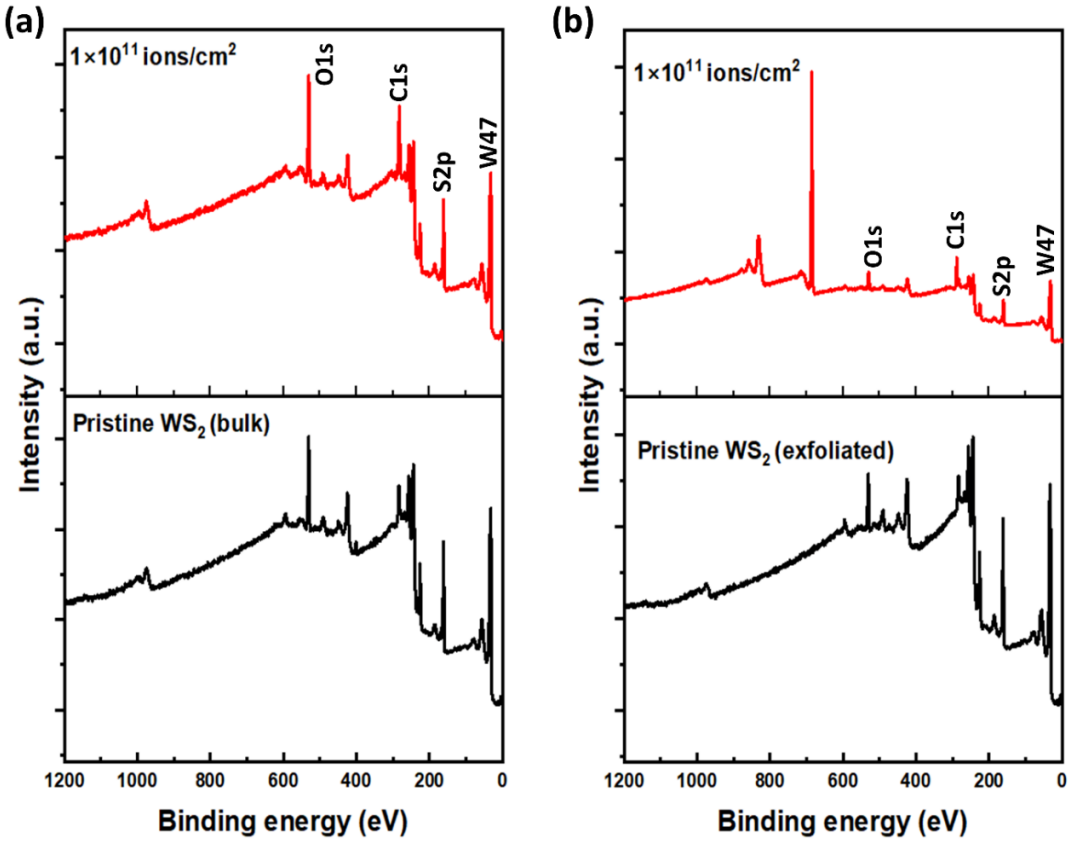

Figure A9: XPS survey scans of (a) bulk and (b) exfoliated WS_2 with 0.85 GeV U^{28+} ions at fluence 1×10^{11} ions/cm^2.

A11: Deconvoluted plots of steady state PL spectra of bulk and exfoliated WS_2 before and after irradiation at a fluence of 1×10^{11} ions/cm^2, acquired at specific temperatures

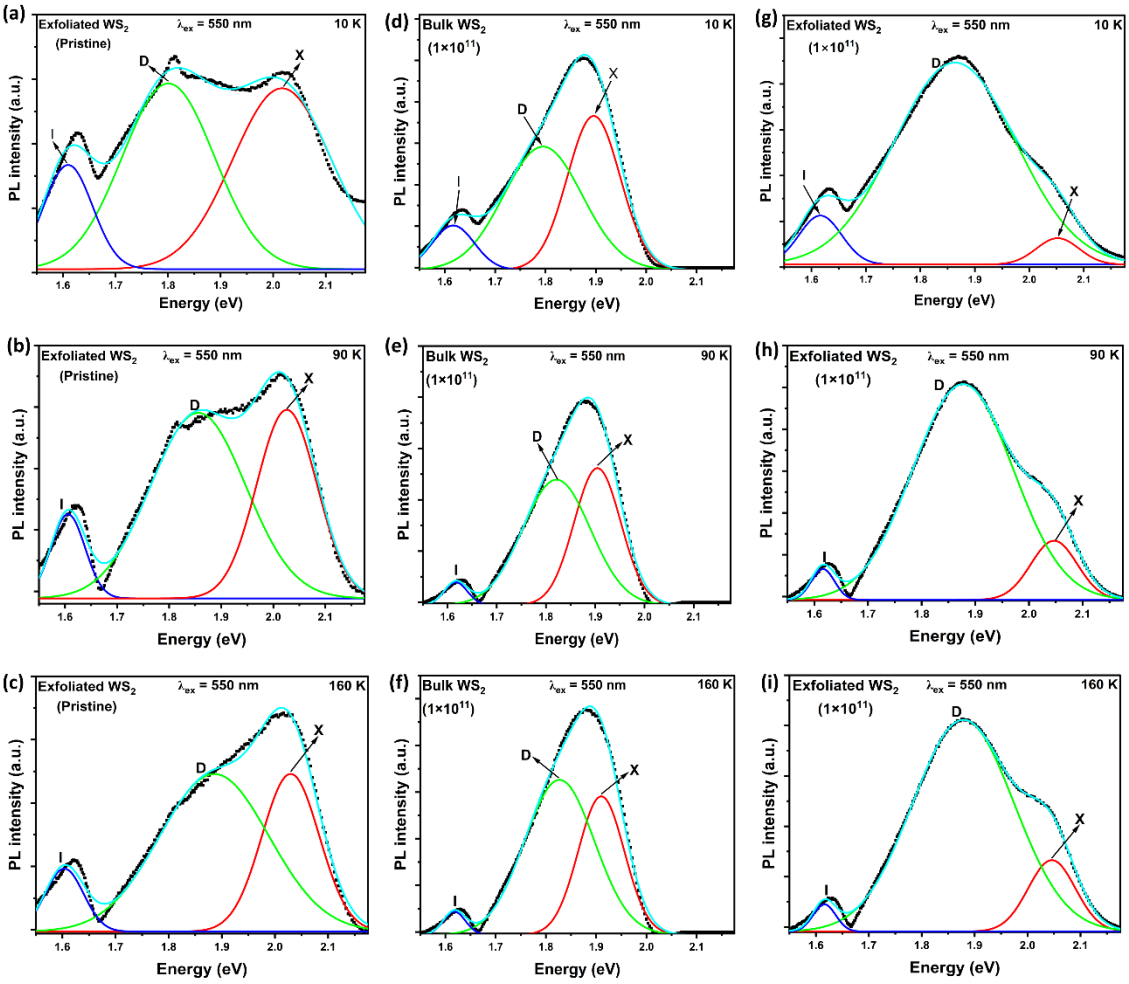

Figure A10: Deconvoluted plots (using the Gauss fitting function) of (a-c) exfoliated WS_2 without irradiation (pristine), and (d-f) bulk and (g-i) exfoliated WS_2 after irradiation at a fluence of 1×10^{11} ions/cm^2, acquired at 10 K, 90 K, and 160 K, respectively.

A12: Bar plot of power law index, *m*, against different shear rate ranges of un-irradiated WS_2 and γ-irradiated at 10 kGy and 35 kGy

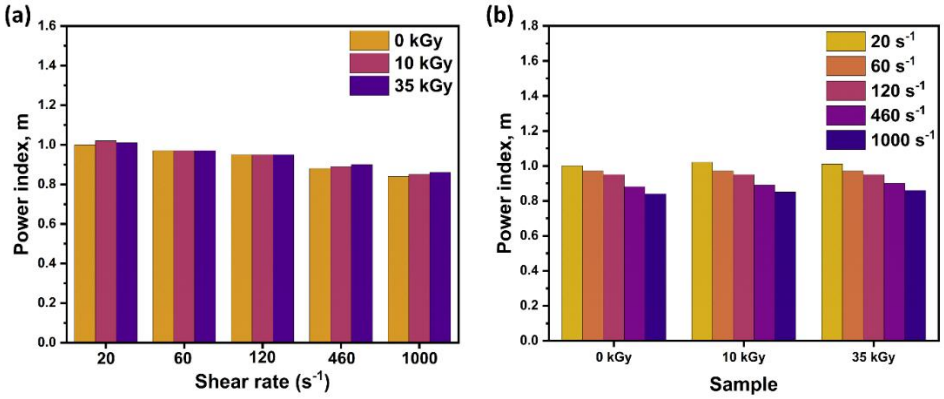

Figure A11: Bar plot of (a) power law index, *m* against different shear rate ranges, (b) showing variation of power index *m* of exfoliated WS_2 system both before and after γ-irradiation till 20 s^{-1}, 40 s^{-1}, 60 s^{-1}, 120 s^{-1}, 460 s^{-1}, and 1000 s^{-1}.

A. Journal articles:

1. **Bhupali Deka**, D. Mohanta, A. Saha, Featuring exfoliated 2D stacks into fractal-like patterns in WS_2/carboxy methyl cellulose nanocomposites, *Surfaces and Interfaces*, 29 (2022) 101727.
2. **Bhupali Deka**, D. Mohanta, V. Naik, and A. Saha, Directing exfoliation, slipping, and corrugation in WS_2 through bubbling with 15 keV He^{2+} ion irradiation, *Physica Status Solidi B*, 260 (2023) 2200598.
3. **Bhupali Deka**, D. Talukdar, D. Mohanta, Effect of 60 MeV nitrogen ion irradiation on few layer WSe_2 nanosystems, *Nuclear Instruments and Methods in Physics Research*, *B*, 554 (2024) 165438.
4. **Bhupali Deka**, D. Talukdar, V. Naik, A. Saha, D. Mohanta, Generating immiscible WC phase in layered WS_2 upon 15 keV C^{2+} irradiation, *Physica Scripta*, 100 (2025) 025931.
5. **Bhupali Deka**, B. Boro, D. Chowdhury, A. Saha, D. Mohanta, Manifested mechanical features of γ-irradiated WS_2 nanosheet-dispersed carboxy methyl cellulose, *Materials Science and Engineering B*, 324 (2026) 118959.

B. Conference Proceeding:

1. **Bhupali Deka**, D. Mohanta, Altered mesopore distribution in exfoliated WS_2 nanosheets with radiation exposure, *Materials Today: Proceedings,* 66 (2022) 3405-3411.

C. Book Chapters:

1. **Bhupali Deka**, D. Mohanta, Low-energy 15 keV He^{2+} and C^{2+} irradiation effects in WSe_2, chapter in the book "Current Trends in Materials Science", to be published by *Springer Nature* (*under review*).
2. A. Medhi, **Bhupali Deka**, D. Mohanta, 22 - Prospects of two-dimensional nanoscale functional materials with relevance in sensing and actuation, in: P. Chakraborty, D. Mohanta (Eds.), Low-Dimensional Materials, Systems and Applications, Volume 1, Woodhead Publishing, (2026) 675–706.

D. Other publication:

1. K. Doloi, D. Mohanta, **Bhupali Deka**, Enhanced and efficient electrochemical detection of IgG by UiO-66 metal organic framework (MOF) upon 60 MeV N^{5+} swift ion impact, *Microchemical Journal*, 208 (2025) 112489.

List of Conferences/Workshops attended

1. Presented **poster** at 29th National (Virtual) Conference on Condensed Matter Physics "(CMDAYS2021)" held on December 10-12, 2021, at the Department of Physics, Central University of Jharkhand, Ranchi, Jharkhand.
2. Presented **poster** at 30th National Conference on Condensed Matter Physics "(CMDAYS2022)", December 14-16, 2022, Department of Science and humanities, National Institute of Technology, Nagaland, India.
3. Presented **oral** at the 7th International Conference on Ion Beams in Materials Engineering and Characterization (IBMEC 2022) November 16-19, 2022 Inter-University Accelerator Centre, New Delhi, India.
4. Presented **oral** on ICNP 2023-International Hybrid Conference on Nano Structured Materials and Polymers, May 12-14, 2023, Mahatma Gandhi University, Kottayam, Kerala, India.
5. Presented **poster** at 7th International Conference on Nanostructuring by Ion Beams (ICNIB 2023), during 2-4 November at UPES, Dehradun.
6. Presented **oral** at 2nd International Conference on Recent Trends in Materials Science & Devices 2023 (ICRTMD-2023), 29-31 December 2023 organized by Research Plateau Publishers & Sat Kabir Institute of Technology & Management Bahadurgarh, Haryana, India.
7. Presented **poster** at 31st National Conference "Condensed Matter Days, CMDAYS 2023", held on January 22nd – 24th, 2024, at Tezpur University, Assam.
8. Presented **poster** at the Fourth International Conference on Material Science (ICMS 2024), January 31st – February 2nd, 2024 organized by the Department of Physics, Tripura University.
9. Presented **oral** at XIV Biennial Conference of Physics Academy of the North-East, held on November 12-14, 2024, at Tezpur University, Assam.
10. Attended "Hands-on training program on Computation, Fabrication, and Characterization of Devices and Systems" under **DST STUTI** during June 13-19, 2022 organized by the Department of Electronics and Communication Engineering, Tezpur University, India.
11. Attended National Seminar cum Workshop on Quantum Materials and Devices, 3-4 March 2025 at Tezpur University, India.